



Impact of the Position and Length of the Lid Moving Part on Mixed Convection in Porous Cavities

Liamena Hassinet^{1,2*} , Mohamed Si-Ameur² 

¹ Department of Science and Technics, University Center of Mila, Mila 43000, Algeria

² LESEI Laboratory, Department of Mechanical Engineering, University Batna 2, Batna 05000, Algeria

Corresponding Author Email: l.hassinet@centre-univ-mila.dz

Copyright: ©2025 The authors. This article is published by IIETA and is licensed under the CC BY 4.0 license (<http://creativecommons.org/licenses/by/4.0/>).

<https://doi.org/10.18280/ijht.430208>

ABSTRACT

Received: 10 February 2025

Revised: 26 March 2025

Accepted: 9 April 2025

Available online: 30 April 2025

Keywords:

lid-driven flow, porous cavity, vortex formation, Darcy number, Richardson number, heat transfer enhancement, finite volume method, numerical simulation

This study explores mixed convection in a square porous cavity, highlighting the dominant influence of a lid moving part (LMP) on flow dynamics and heat transfer. Numerical simulations, based on the Finite Volume Method, reveal that both the position and length on the LMP strongly affect vortex formation on and thermal performance. When the LMP is shifted and elongated, it induces multiple vortices that reduce the average Nusselt number. However, optimal configurations such as placing the heated wall on the right and adjusting the LMP location can significantly enhance heat transfer. A key finding is that mechanical forcing from the LMP outweighs buoyancy effects, especially at lower Darcy numbers, where heat transfer increase up to 9.5 fold. The study underscores the non-monotonic influence of LMP geometry, and the interplay between Darcy and Richardson numbers in shaping temperature gradients and flow behavior within porous media.

1. INTRODUCTION

The fluid motion during mixed convection in a lid-driven cavity, is induced by both buoyancy forces arising from temperature gradients, and the shear force exerted by the movement of one or more cavity walls. For many years, there has been extensive research on mixed convection in lid-driven cavities that has resulted in many benefits for engineering and industrial applications [1-7]. Applications of mixed convection in porous media have become increasingly important in engineering and industrial uses, including cooling/heating buildings, room ventilation, drying technologies, geothermal systems, food processing, nuclear and chemical reactors [8-11].

A particular implementation occurs when a cavity is driven by a moving wall, and since then a significant number of research has emerged on numerical simulations [12, 13] and theoretical ones Aldoss et al. [14]. The literature is more inclined to numerical research than experimental [11].

During the past two decades, a renewed deep interest on mixed convection resulting from the mobility of one wall of porous cavities can be seen [15-18]. Different thermal conditions at the boundary of the cavity have been conducted in various research. Numerical study was carried out with a partially heated porous cavity and it has verified that the most efficient heat transfer happens when the left wall is being exposed to the hot temperature Oztop [19]. According to Kandaswamy et al. [20] findings, mixed convection influences the temperature field as the number of Prandtl increases. However, conduction plays a key role in low Prandtl numbers. However, mixed convection influences the temperature field as the number of Prandtl increases. The effect of uniform or

linearly heating side walls has been analyzed by Basak et al. [21]. It has found that for linearly heated left wall, Nusselt number at the top wall increases, and a non-monotonic trend can be seen in the Nusselt number on the left side for higher Pr and Da numbers. Karimipour et al. [22] evaluated the influence of the lid's movement type. The upper lid is given a sinusoidal motion. It was found that in the stationary periodic state, the highest value of Richardson number is associated with the lowest value of the oscillation's amplitude.

The study of mixed convection generated by two-sided lid-driven is introduced by numerous researchers. Maghsoudi and Siavashi [23] and Muthamilselvan et al. [24] focused on studying mixed convection within a square porous cavity with horizontal walls moving in either the same or opposite direction. Chattopadhyay et al. [25] treated the problem in the porous cavity by moving vertical walls differentially heated in three different directions. Rajarathinam et al. [26] have used an inclined porous cavity. It was noted that the Nusselt number and convection behavior were significantly affected by the direction of the moving walls. Alsabery et al. [27] studied the effect of the moving walls and found that it impacts the increase of the average Nusselt number at the heated surface while the undulations number decreases the intensity of thermal transmission. Tiwari et al. [28] investigated the effect of the direction of motion of the left and the right moving walls on the flow and thermal behavior. According to research, the direction of the walls in motion and the Richardson number are crucial.

Using four moving faces, Bagai et al. [29] studied the mixed convection in porous cavity that is heated by sinusoidal temperatures by utilizing the stream function and vorticity formulation. Bagai et al. [30] investigated mixed convection

in a differentially heated porous cavity, the temperatures are constants and the four walls are moving in opposite directions. It was discovered that the streamline contours change the nature from vertical to horizontal when the direction in which the walls move is changed.

The originality of the present study lies in its novel approach to exploring mixed convection in porous cavities, with a particular focus on the position and length of the lid's moving part (LMP) within a square cavity. While prior research has predominantly examined the displacement of entire or partial walls, this work introduces a unique configuration where only a segment of the lid moves. This approach, inspired by the study of Mondal et al. [31], is especially relevant in situations where spatial constraints preclude the movement of the entire wall.

In other terms, this paper expands on the existing literature by investigating the impact of varying both the position and length of the LMP on convection and thermal characteristics within the cavity. Unlike previous studies, which have focused mainly on the movement of either the entire lid or portions of it without addressing the influence of the LMP's position and length, this study provides a comprehensive understanding of how these parameters affect flow dynamics and heat transfer in a porous cavity under mixed convection conditions.

This research's main goal is then to fill a significant gap in the literature by generating new insights into the effects of LMP position and length on mixed convection. In doing so, the study aims to provide valuable data that is currently lacking, enabling a more complete understanding of flow behavior and temperature distribution within porous cavities. This work not only expands the field of study on mixed convection in porous cavities but also introduces new variables such as the LMP's position and length that could greatly enhance the understanding and optimization of thermal processes in various industrial applications.

To achieve these objectives, the research explores the role of the LMP's position and length, investigate the influence of Richardson and Darcy numbers, and identify optimal configurations for thermal performance in porous cavity systems.

2. PROBLEM FORMULATION AND GOVERNING EQUATIONS

Figure 1(a) illustrates the schematic of the investigated problem, which is a square porous cavity where the right and the left sides of the cavity are maintained at the hot and cold constant temperatures respectively, and the horizontal walls are insulated. Because of the assumption, a part of the top wall [ab] moves from right to left at a speed U_0 .

Figure 1(b) shows the three locations of this moving part, in left, middle and right. For each position, moving part has three different lengths: $l_p = L_0/4, L_0/3$ or $L_0/2$.

The present study is performed for a steady laminar flow in porous media saturated with an incompressible fluid. The Boussinesq approximation is used to model the buoyancy force and to assume that there is no distinction between the fluid and solid temperatures in the porous media, the local thermal equilibrium law defined in Nield and Bejan [32] is employed in the investigation. However, this study does not include Forchheimer's inertia term because it is focused on mixed convection in a porous medium with moderate Reynolds numbers, where the drag effect is thought to be less important Ferziger and Peric [33].

Based on these assumptions and using Brinkman-extended Darcy model cited in Vafai and Tien [12], the equations of mass, motion, and energy conservations in a dimensionless form for modelling mixed convection in a porous lid-driven cavity are mentioned below:

$$\frac{\partial U}{\partial X} + \frac{\partial V}{\partial Y} = 0 \quad (1)$$

$$U \frac{\partial U}{\partial X} + V \frac{\partial U}{\partial Y} = -\frac{\partial P}{\partial X} + \frac{1}{\text{Re}} \left(\frac{\partial^2 U}{\partial X^2} + \frac{\partial^2 U}{\partial Y^2} \right) - \frac{1}{\text{Re Da}} U \quad (2)$$

$$U \frac{\partial V}{\partial X} + V \frac{\partial V}{\partial Y} = -\frac{\partial P}{\partial Y} + \frac{1}{\text{Re}} \left(\frac{\partial^2 V}{\partial X^2} + \frac{\partial^2 V}{\partial Y^2} \right) - \frac{1}{\text{Re Da}} V + \text{Ri} \theta \quad (3)$$

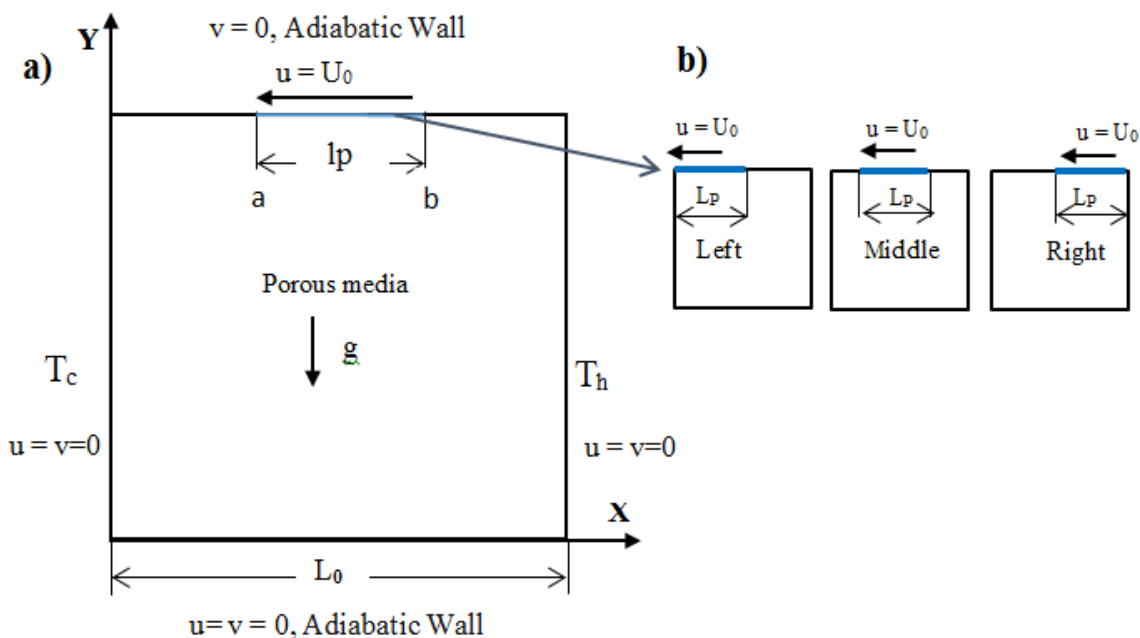


Figure 1. a) Physical system, b) Positions of the LMP

$$U \frac{\partial \theta}{\partial X} + V \frac{\partial \theta}{\partial Y} = \frac{1}{\text{Re} \cdot \text{Pr}} \left(\frac{\partial^2 \theta}{\partial X^2} + \frac{\partial^2 \theta}{\partial Y^2} \right) \quad (4)$$

To describe the boundary conditions, the cavity is designed to cool to the left and heat to the right sides, and it is insulated at both the top and bottom. The non-slip condition is applied thus the fluid velocities are zero ($U=V=0$) at adjacent walls except for the moving part of the lid (LMP) which has a velocity of $U=-1$.

The Nusselt number is commonly used to quantify the cavity's heat transfer characteristics. The average and local Nusselt numbers along the right wall can be calculated using these equations:

$$\text{Nul} = \left. \frac{\partial \theta}{\partial X} \right|_{X=1} \quad (5)$$

$$\text{Nu}_{avg} = \int_0^1 \text{Nul} \times dY \quad (6)$$

The dimensionless parameters and variables mentioned below are used in Eqs. (1) to (6):

$$L_p = \frac{lp}{L_0}, \quad X = \frac{x}{L_0}, \quad Y = \frac{y}{L_0}, \quad U = \frac{u}{U_0}, \quad V = \frac{v}{U_0},$$

$$P = \frac{p}{\rho U_0^2}, \quad \theta = \frac{T - T_c}{T_h - T_c}, \quad Da = \frac{K}{L_0^2}, \quad \text{Pr} = \frac{\nu}{\alpha},$$

$$\text{Ri} = \frac{Gr}{\text{Re}^2}, \quad \text{Re} = \frac{U_0 L}{\nu}, \quad Gr = \frac{g \beta (T_h - T_c) L^3}{\nu^2}$$

where, α is the thermal diffusivity,

$$\alpha = \frac{k_{eff}}{\varepsilon \rho_0 c_{pf}}$$

With ρ_0 refers to the density of the fluid at a temperature $T=0$ and c_{pf} denotes the specific heat of the fluid. Air was chosen for the working fluid $\text{Pr}=0.71$ in this study, and $Gr=10^4$ was set as the Grashof number for all calculations.

3. NUMERICAL APPROACH AND VALIDATION

Using Fortran-developed code and appropriate boundary conditions, the dimensionless partial differential Eqs. (1) to (4)

are solved numerically. The discretization of the Eqs. (1) to (6) is done using the finite volume approach and the solution is obtained iteratively using the SIMPLE algorithm Patankar [34] and the Incomplete LU decomposition algorithm Ferziger and Peric [33]. The ultimate solutions are attained when the maximum residual values are less than 10^{-9} .

In our previous study Hassinet and Si-Ameur [35] on natural convection, this algorithm has been thoroughly validated. Furthermore, a case of mixed convection flow in a square porous cavity, in which the left wall ascends and cools at a low temperature, while the right wall descends and heats at a high temperature has been validated according to Chattopadhyay et al. [25].

In Table 1, we present the findings and the published ones using vorticity (ζ), temperature (θ), and Stream function (ψ) at the center of the cavity. The table shows that both results are in good agreement.

We examined also the flow structure in a cavity that is similar to the case 1 reported by Chattopadhyay et al. [25]. To evaluate the precision of the numerical method that is currently in effect, Figure 2 shows excellent consistency with the work regarding isotherms and streamlines contours for various Richardson numbers. The current code's confidence in studying this problem is confirmed by these findings, as a result.

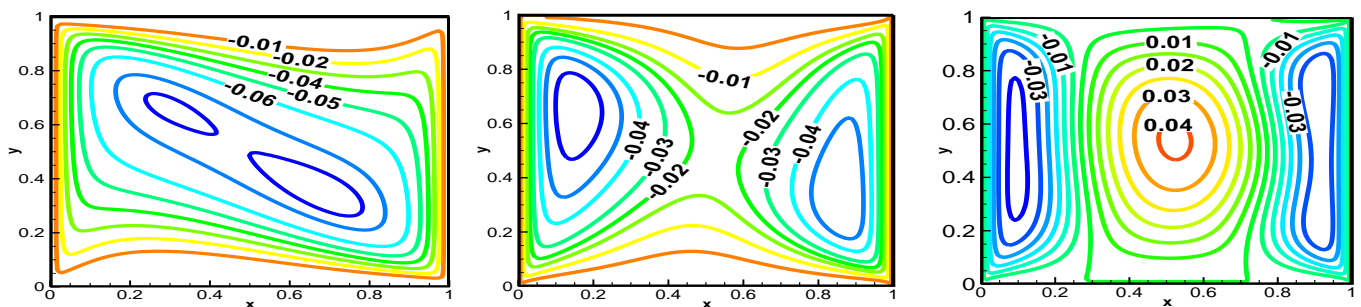
A grid refinement study was conducted, as presented in Table 2, to verify that the obtained solution is independent of the mesh resolution for the problem analyzed in this study for U_{max} , V_{max} and Nu_{avg} for $\text{Ri}=1$ $Da=0.1$ and $L_p=1/4$ on four different grid sizes 104×104 , 111×111 , 121×121 and 171×171 . It has been noticed that the grid size of 121 by 121 is both reliable and of sufficient size. It can be employed to attain grid independence. Subsequently, this grid is employed for all subsequent computations.

Table 1. Comparison of (ψ), (ζ) and (θ) at the cavity center

Da=0.001			Da=0.01	
	Present	[25]	Present	[25]
ψ	0.03091	0.03144	0.22575	0.22887
ζ	0.74526	0.74462	5.38890	5.40229
θ	0.33527	0.33653	0.34006	0.34414

Table 2. Grid independency test for $\text{Ri}=1$, $Da=0.1$ and $L_p=1/4$

Grid	U_{max}	V_{max}	Nu_{avg}
104×104	0.910441	0.884436	3.503490
111×111	0.949978	0.901131	3.480339
121×121	0.95685	0.909254	3.473605
171×171	0.956997	0.909996	3.470480



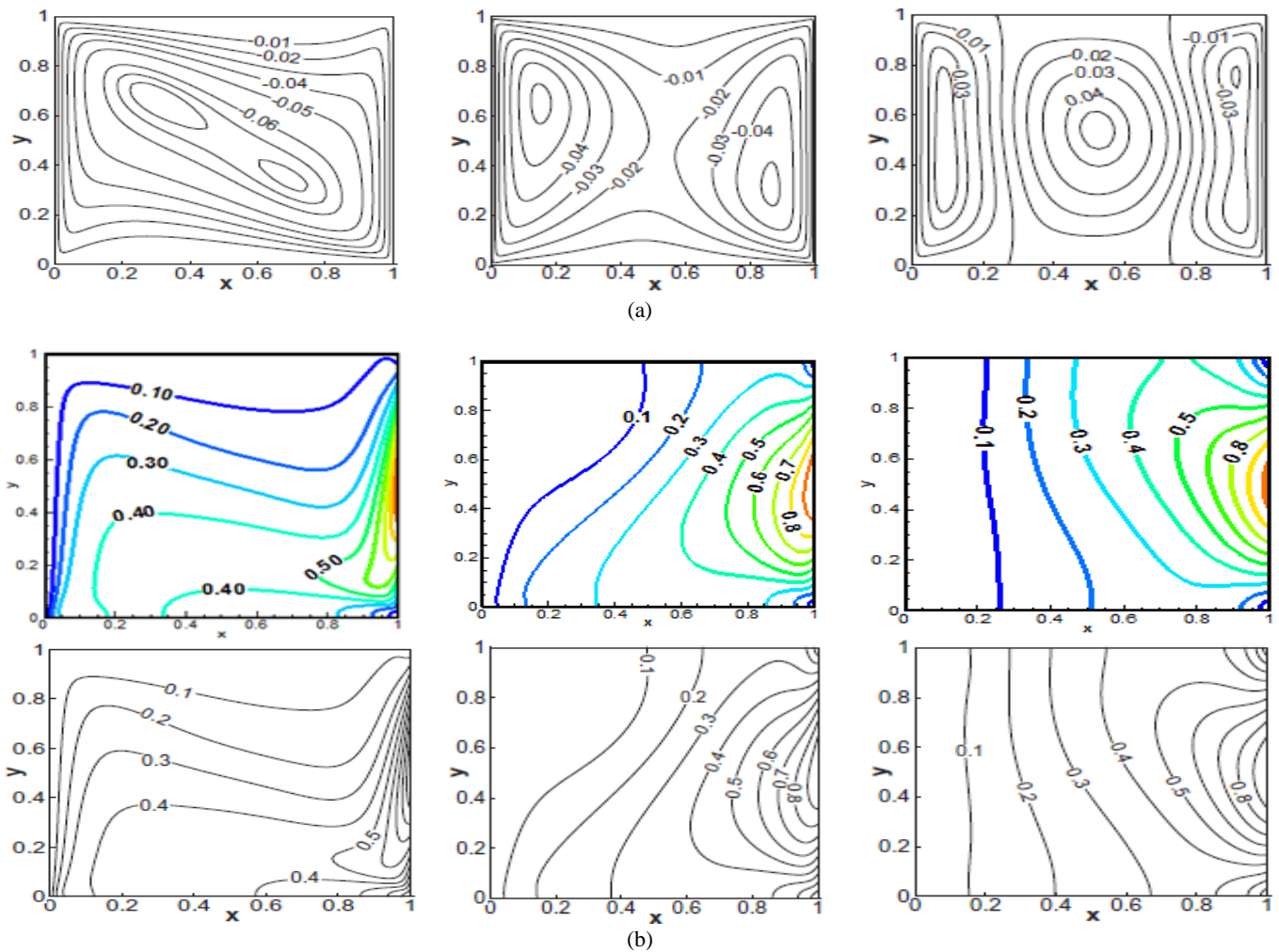


Figure 2. Streamlines (a) and Isotherms contours (b) comparison, present and [25] for $Ri=0.1, 1$, and 10 at $Da=0.01$

4. RESULTS AND DISCUSSION

The results obtained reveal the crucial role of the position and length of the movable part of the lid (LMP) of the studied cavity on highlighting the mixed convection characteristics. Position is left, middle or right and length is $L_0/4$, $L_0/3$ or $L_0/2$. A differentially heated cavity study using 108 simulations examines the relevance of the Richardson number Ri ($0.1 \leq Ri \leq 10$) and Darcy number Da ($1e-7$ to $1e-1$).

This work focuses on taking into account the partial movement of the wall by dividing the lid of a cavity into stationary and mobile parts.

Figure 3 shows how the length of the LMP affects the streamlines and isotherms for middle position of the moving part with Richardson number Ri equals $0.1, 1$, or 10 at Darcy number Da equals 0.1 . It can be seen that as the Ri number rises, the flow strength lowers, and as the length of the LMP rises, the flow strength rises too. When $Ri=0.1$, configurations depict a primary recirculating eddy of the size of the cavity created by the lid. It suggests that the mechanical influence of the sliding part of the lid surpasses the buoyancy effect. This leads to a high sensitivity of the flow characteristics to the length of the moving part. Additionally, there are secondary vortices situated at the right top corner.

There is also a smaller one at the lower left side for $L_P=1/2$. The length has a significant impact on the additional vortices. At $Ri=1$, the second-order vortices are moved from the right top corner ($Ri=0.1$) to the left top one.

For $Ri=10$, a greater dominance of the buoyancy force, leading to the creation of smaller vortices than in the two cases of $Ri=0.1$ and 1 . Significant temperature variations can be seen in the left side of the cavity are deduced from the grouped isotherms near this region in the case for of $Ri=0.1$ and 1 . But in the case $Ri=10$, the isotherms have expanded inside the cavity due to buoyancy forces.

For every length of LMP, at $Da=0.1$, Figure 4 depicts the streamlines and isotherms for the left, middle, and right positions for $Ri=1$. In left case configurations, the primary circulation takes up most of the cavity and its strength increases with length L_P . For $L_P=1/2$ the stream function has a maximum value $\psi_{max}=1.233$. On the left top side of the cavity in the middle case configurations, a secondary vortex is formed. It is developed for the right case configurations with lengths of $L_P=1/3$ and $L_P=1/4$. From the ψ_{min} values shown in Figure 4, it is evident that this vortex is formed due to the contrast between the forces caused by buoyancy and lid motion. Its development is enhanced by increasing LMP length.

The isotherms display a straight distribution in the left region of the cavity, due to the buoyancy force being more dominant in the right region. By approaching the LMP to the hot surface (middle or right position), the transfer mode approaches the forced convection for all configurations except for the one where the length of $L_P=1/4$, and the position of LMP is at right.

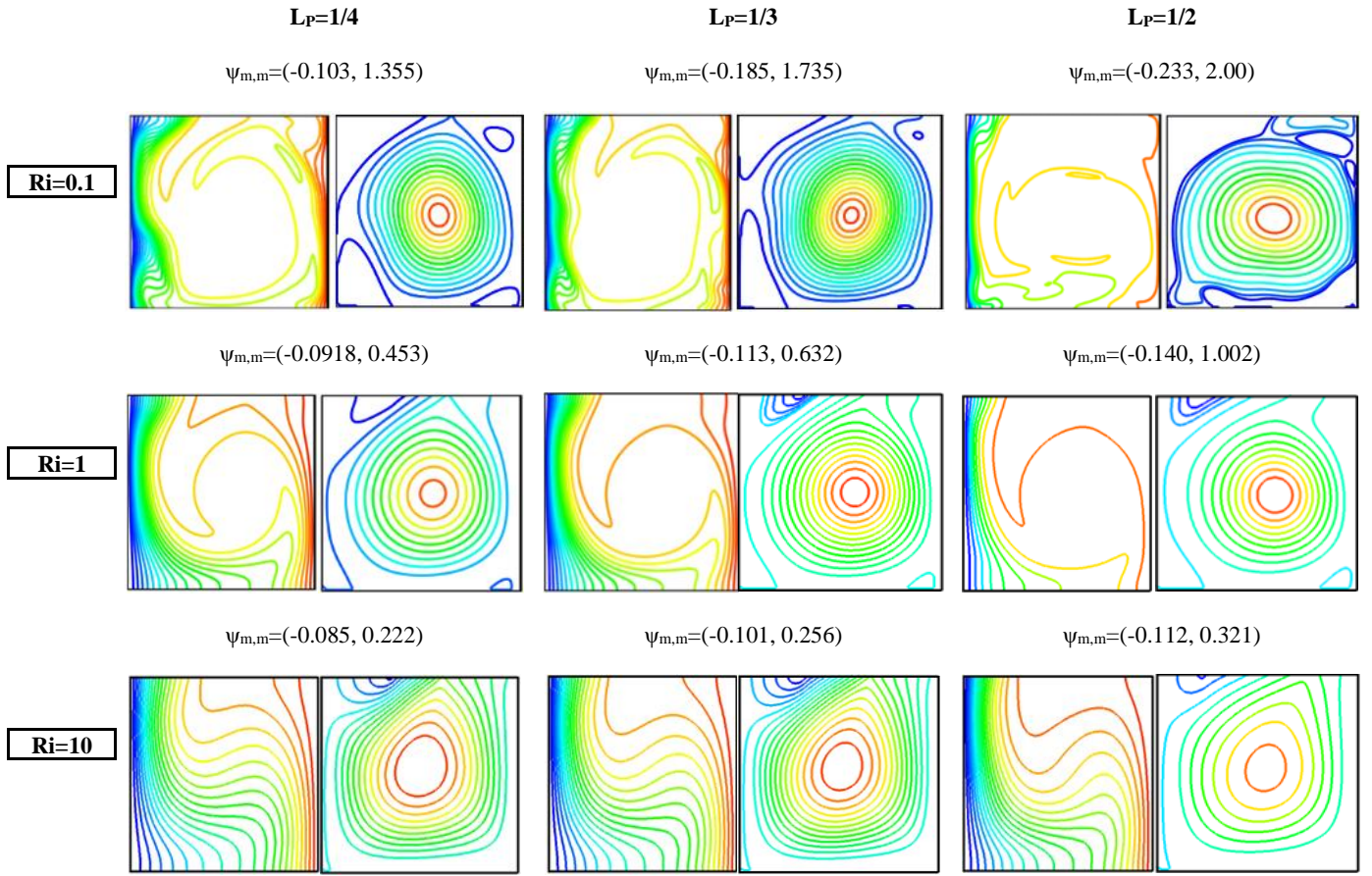


Figure 3. Isotherms (at left) and Streamlines (at right) for middle position of LMP for $L_P=1/4$, $1/3$, and $1/2$ for: Ri; a) Ri=0.1, b) Ri=1 and c) Ri=10; Da=0.1

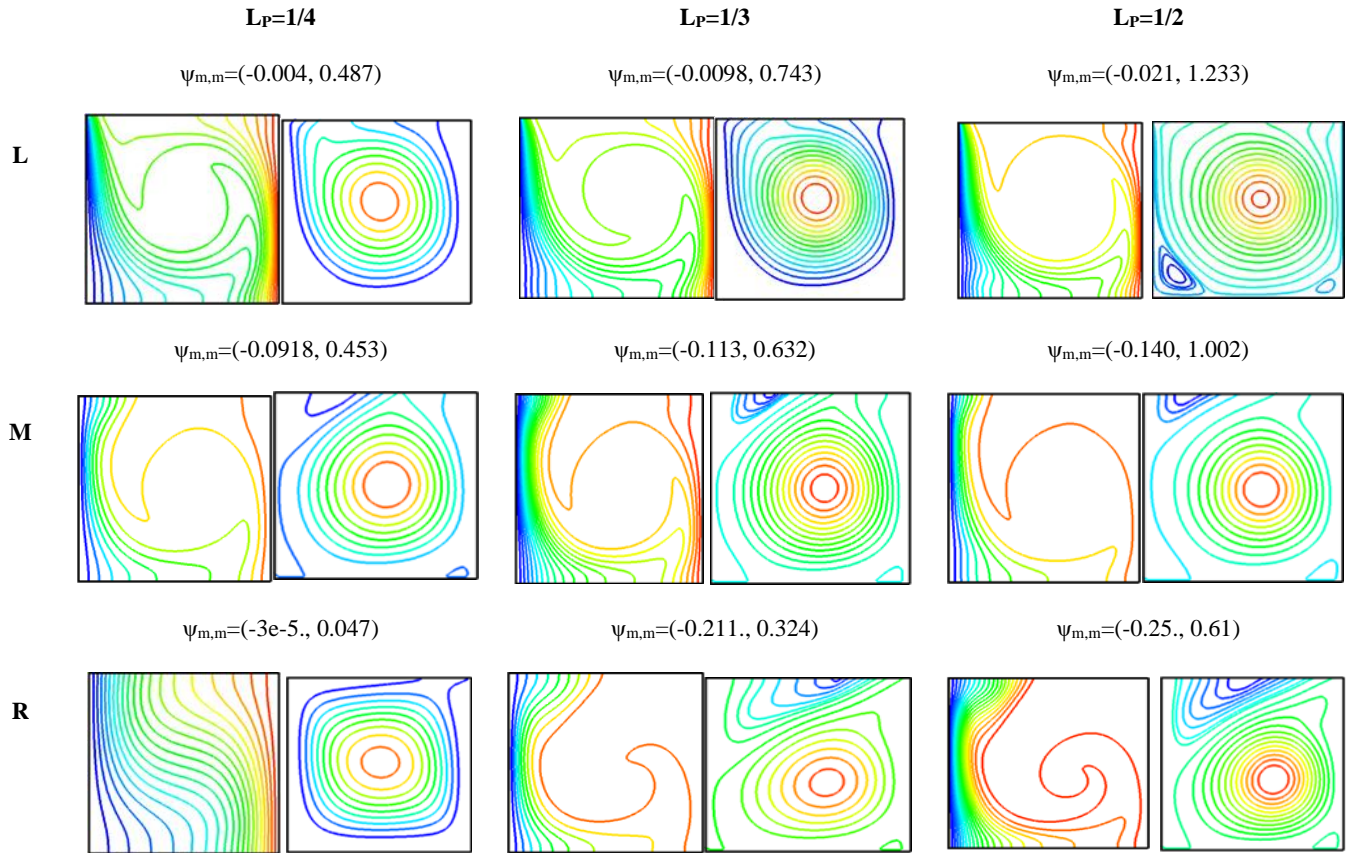


Figure 4. Isotherms (at left) and Streamlines (at right) for different L_P and different LMP's positions at Da=0.1 Ri=1

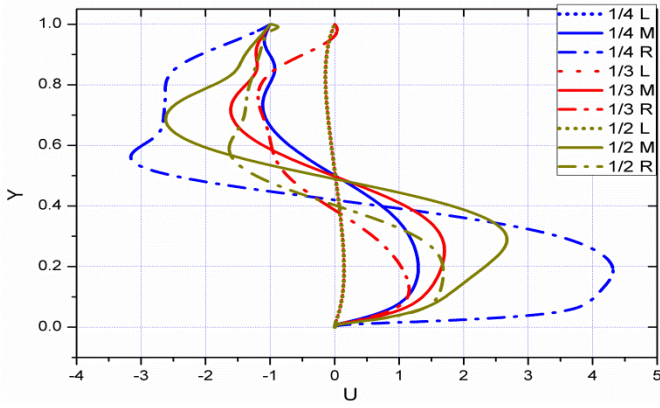


Figure 5. Horizontal velocity profiles along the vertical center line $X=0.5$ at $Ri=1$, for $Da=0.1$

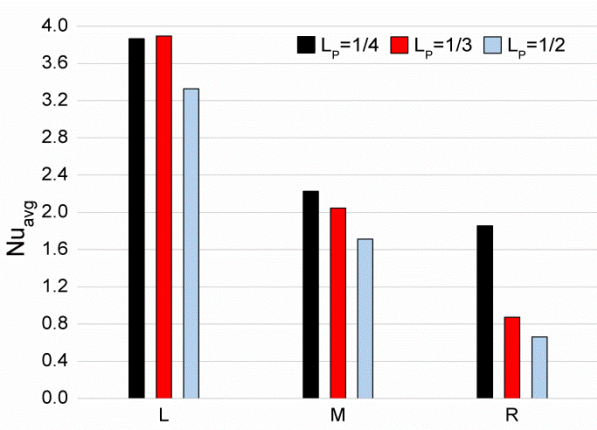


Figure 6. Nu_{avg} for different Lid's moving part positions and lengths at $Ri = 1$, for $Da = 0.1$

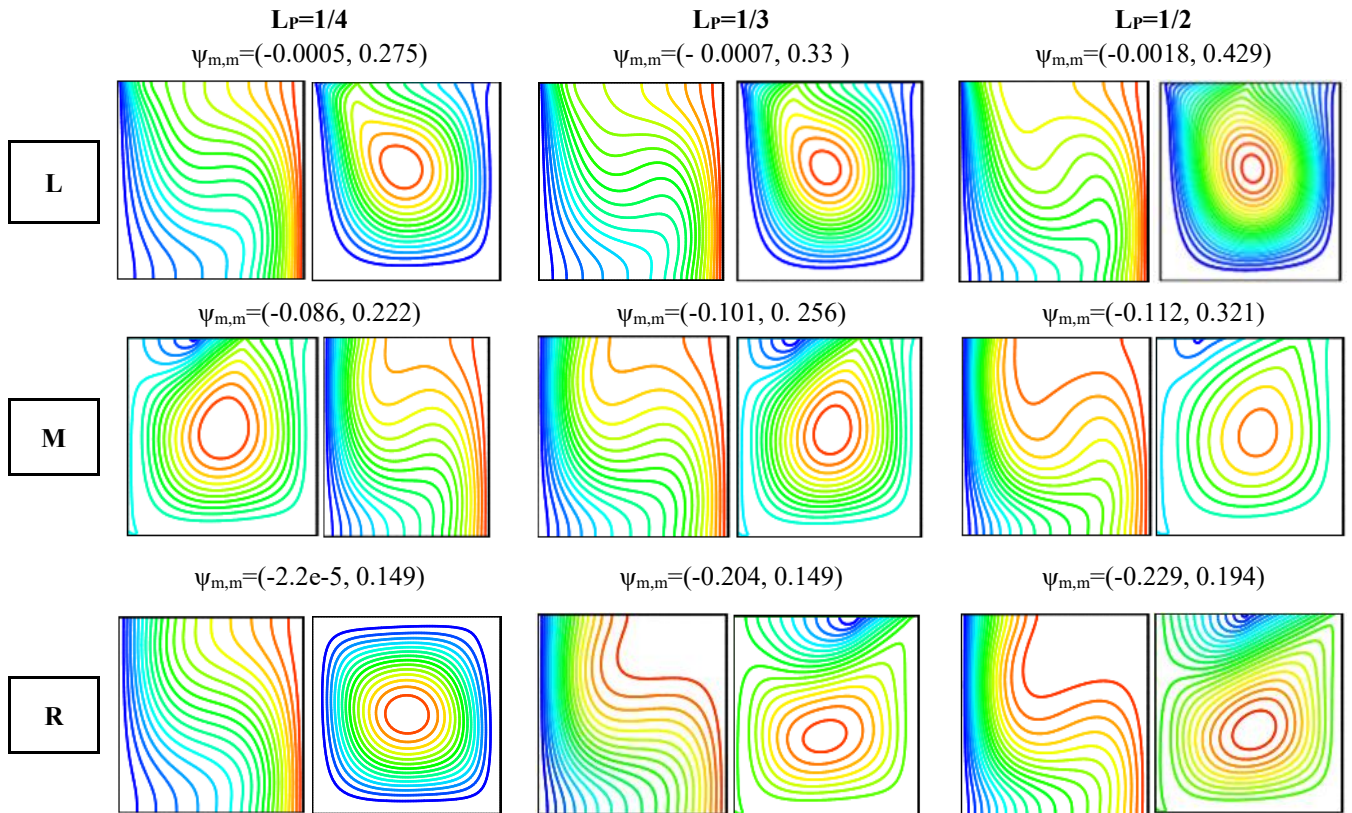


Figure 7. Isotherms (at left) and Streamlines (at right) for different L_p and different LMP's positions at $Da=0.1$ $Ri=10$

Figure 5 illustrates X-velocities in the mid-X plane for all LMP configurations (lengths and positions) at $Da=0.1$ and $Ri=1$. It's evident from this figure that velocities for all lengths of LMP at left location are getting close to each other, almost superimposed, and they are getting close to zero values, whereas the velocities values for middle positions of LMP are positive in the lower half of the cavity, while they are negative in the upper half with zero values located at the center of the cavity.

This has especially noticeable in the middle of the field caused by the resultant forces included the inertia force near the left wall and the buoyancy force near the right wall, with $Ri=1$ which lead to this behavior.

The amplitudes of velocities of middle positions of LMP are significant according to length. In the right positions of LMP there is no similar phenomenon; the high velocities values are for length $L_p=1/4$ at right, the amplitudes of velocities are positive in the lower part ($Y \leq 0.4$) and negative in the upper part ($Y \geq 0.4$) of the cavity.

Velocities are positive in the lower part ($Y \leq 0.4$) and negative in the upper part ($Y \geq 0.4$) of the cavity.

Figure 6 illustrates that at $Da=0.1$, it becomes evident that the LMP's positions and lengths have distinct effects when comparing the mean Nusselt numbers for $Ri=1$.

Specifically, the highest values of Nu_{avg} are always obtained by positioning LMP to the left, while positioning it to the right leads to lower values. Due to the direct interaction between the cold stream and the portion in motion, and the Nu_{avg} calculated on the right side of the cavity results in a significant increase in the thermal gradient in the left configurations. While for the right configurations, the cold stream carried by the LMP does not arrive at the hot wall. An increase in the length of L_p leads to the development of more vortices, resulting in significantly lower Nu_{avg} results.

Figure 7 displays, at $Ri=10$ and $Da=0.1$, isotherms and streamlines for various L_p and positions of LMP. An increase in the Ri number causes a more dominant buoyant force that decreases the strength of the primary recirculation flow. LMP length too has a great influence on the vortices; this effect can be seen with the case of the right position for $L_p > 1/4$, in which the strength of the vortices recirculation flow is higher than that of the primary recirculation. As evidenced by this case, the cavity contains two recirculation cells, one at the top rotating clockwise and the other rotating counter-clockwise, forced convection takes over the first, and floatability forces take over the second. This is due to the competitive nature of buoyant and inertial forces being reduced.

Isotherms' clustering behavior decreases when compared to $Ri=1$, and the majority of the temperature within the cavity is elevated.

Figure 8 depicts x-velocities along the vertical center line $X=0$ at $Da=0.1$ and $Ri=10$. The phenomenon shown in this figure differs from that in Figure 5, velocities for lengths L_p at left location are diverging between each other in the lower half of the cavity with positive values, and they are coming closer to each other in the upper half with negative ones. For right location of LMP velocities values are coming closer to each other between $0.3 < Y < 0.65$ and they vary between them outside this area.

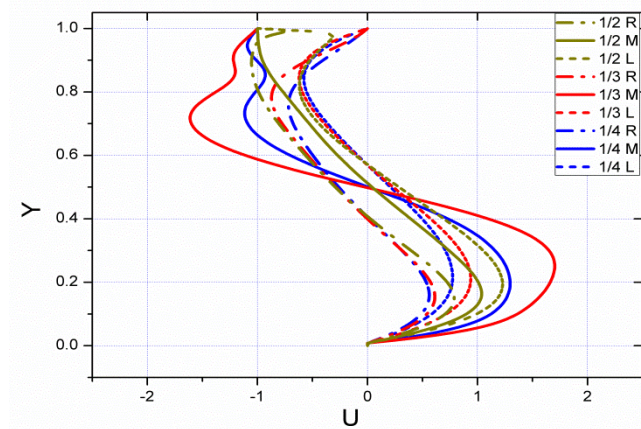


Figure 8. X velocity along the cavity's middle vertical line for different LMP's positions at $Ri=10$ and $Da=0.1$

The configurations and velocity profiles are significantly affected by the plot line passing through vortices. It can also be observed that LMP setup has lower velocity values for the middle positions, which Y range from 0.45 to 0.57.

For $Ri=10$, $Da=0.1$, the lengths L_p (1/3, 1/2) in right configurations has the lowest Nu_{avg} values, according to Figure 9. The value of Nu_{avg} is higher when the moving part is positioned to the left. When the length of the movable part is increased, positioning it to the left or in the middle causes a slight decrease in its value. The lowest values of Nu_{avg} are obtained for the right position for the long lengths, $L_p=1/3$ or $L_p=1/2$, because the convection heat transfer mechanism almost stops in these cases which imply that a quasi-conduction regime has been established.

Figure 10 depicts the streamlines and temperature contours for $L_p=1/4$ at the left position, as calculated for various Richardson and Darcy numbers. A key feature of a lid-driven two-dimensional cavity is the presence of a main recirculating eddy that is the same dimension as the cavity created by the leftward motion of the lid. The flow dynamics and temperature

distribution within the cavity are then shaped by the movement of the lid, which induces a primary recirculating eddy. This eddy, or vortex, is a critical feature of the flow, occupying almost the entire cavity. The size of the eddy is comparable to that of the cavity itself, and it is generated predominantly by the motion of the left portion of the lid. The formation of this primary vortex is a direct result of the shear forces exerted by the lid on the fluid, causing it to circulate within the confined space. The presence of this large eddy has significant implications for the temperature distribution within the cavity.

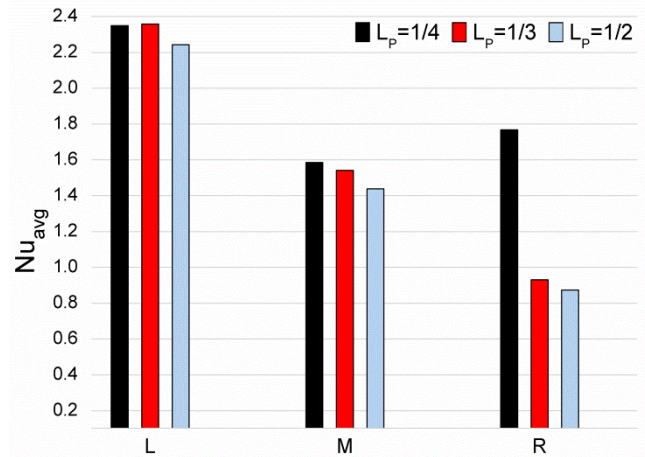


Figure 9. Average Nusselt number for different Lid's moving part positions and lengths at $Ri=10$ and $Da=0.1$

The presence of grouped isotherms near the right side of the cavity suggests the occurrence of significant horizontal temperature gradients in this area. There are only minor temperature differences inside the cavity due to weak temperature gradients in the rest area caused by the mechanically driven circulations.

The flow slowly decreases as the number of Darcy decreases, with the exception of the upper area where the effect slows down. The flow eventually ceases in the most of the cavity as the permeability of the medium gets close to extremely insignificant values of the Darcy number. Also, it is clear when the Da value lowers, the convection heat transfer mechanism significantly slows down, causing the isotherms to align practically parallel to the vertical walls. This indicates the quasi-establishment of a conduction regime. In simpler terms, the temperature changes rapidly over a short distance on the right side of the cavity. This phenomenon can be attributed to the fact that the fluid near the right wall experiences less mixing and more direct interaction with the boundary, leading to the development of sharp thermal gradient.

The horizontal temperature gradients near the right side are indicative of the thermal boundary layer's influence, where conduction dominates and the fluid's temperature adjusts rapidly to match the temperature of the wall. This behavior contrasts with the interior region of the cavity, where the temperature variations are minimal.

The weaker temperature gradients in the central part of the cavity suggest that the fluid is more homogenized in this area, primarily due to the vigorous mixing induced by the recirculating eddy. The mechanical action of the lid-driven flow works to equalize the temperature within the cavity's core, reducing thermal disparities and leading to a more uniform temperature distribution.

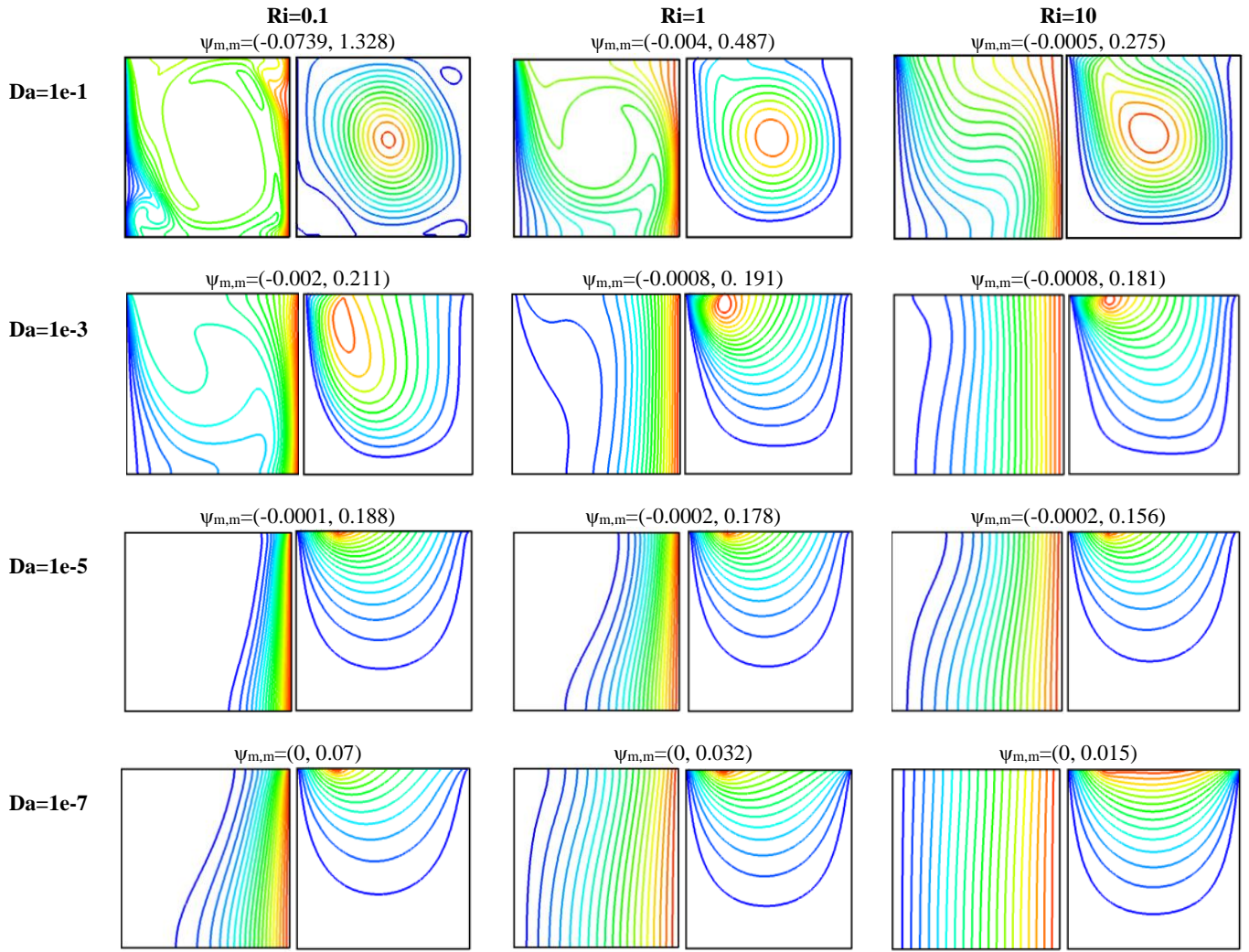


Figure 10. Impact of Da on isotherms and streamlines for $L_p=1/4$ at left position and different Ri

However, the influence of the lid's motion diminishes as one drifts away from the lid and is directed to the bottom of the cavity, where the effects of the primary eddy are less pronounced. In these regions, the fluid experiences weaker circulation, and as a result, the temperature gradients are less steep. The relatively uniform temperature in the cavity's interior is a consequence of this diminished circulation, which fails to induce significant thermal mixing. Consequently, only minor temperature differences are observed in this area.

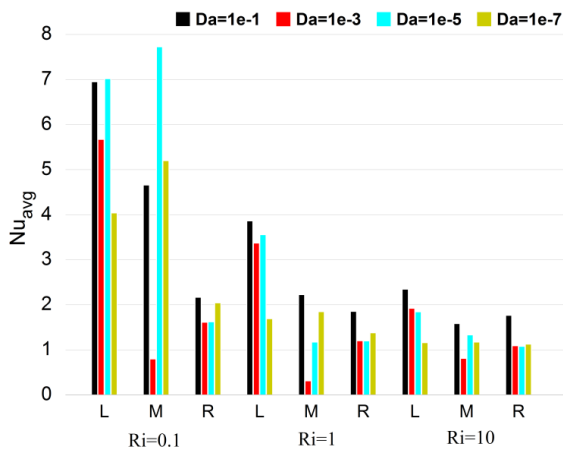


Figure 11. Influence of Da on $L_p=1/4$ for various positions and Ri

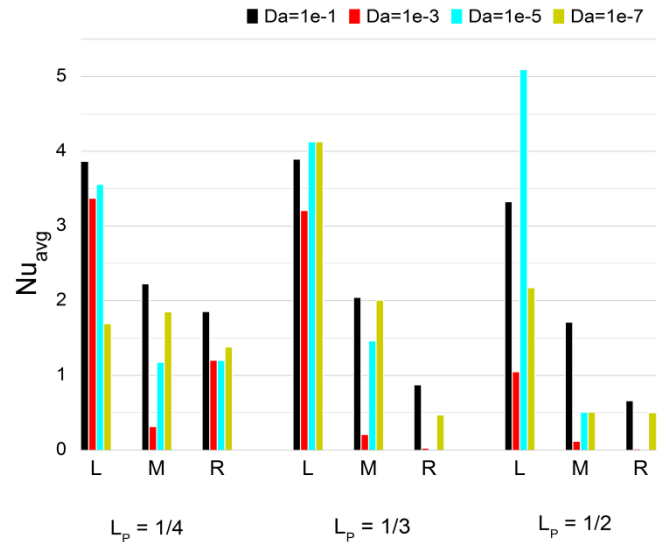


Figure 12. Influence of Da at different L_p for different positions at $Ri=1$

The effect of Darcy number Da and Richardson number Ri on Nu_{avg} for $L_p=1/4$ at different positions can be seen in Figure 11. For all Darcy numbers at the left position, increasing Richardson number causes a decrease of the mean Nusselt number, Nu_{avg} . The same thing occurs for all positions but for only $Da=0.1$. For the middle and left positions, the results from

$Da=10^{-5}$ reveal the highest Nu_{avg} values for $Ri=0.1$. And according to $Da=10^{-3}$, the lowest Nu_{avg} values are found in the middle and right position for the different Ri values.

The impact of Darcy number Da and lengths L_P on Nu_{avg} at $Ri=1$ and different positions is illustrated in Figure 12. The Nu_{avg} value is affected by the flow field variations as the Darcy number decreases.

For a small value of Da and for the same length of LMP, Nu_{avg} can have a larger value as it can have very low by changing only the position of the moving part as seen in this figure. At $L_P=1/2$, Nu_{avg} values in the left position are highest at $Da=10^{-5}$. While the lowest ones are found in middle and right positions. Also, it is shown that for different values of L_P , the number of Nu_{avg} is highest in the left position for different values of Da .

5. CONCLUSIONS

This study provides an analysis on effects of the position and/or length of the left-direction movable unique part of the lid on mixed convection in a square porous cavity and focusing on the impact of Richardson number and Darcy number. The result of the research shows that the parameters of various studied configurations have a reciprocal effect on fluid flow and heat transfer within the cavity.

The findings demonstrate that the Richardson and Darcy numbers are critical in determining velocity profiles and flow configurations, with significant variations observed depending on the presence of vortices and the positioning of lid's moving part. The study also underscores the importance of the length and position of the moving part, showing that these factors can significantly alter the dynamics within the cavity, including the strength of flow and the distribution of temperature.

The key findings of the study include:

- The Richardson and Darcy numbers are critical in determining velocity profiles and flow configurations, with significant variations observed depending on the presence of vortices and the positioning of the lid's moving part.
- The mean Nusselt number is not monotonically related to the position of the moving part, with variations in values depending on the length and position of the moving part.
- The study introduces a novel approach by focusing on the position and length of the lid's moving part within a square cavity, expanding on existing literature that primarily examined the movement of entire or partial walls.
- The research highlights that the parameters of various studied configurations have a reciprocal effect on fluid flow and heat transfer within the cavity.
- The presence of grouped isotherms near the right side of the cavity shows significant horizontal temperature gradients, while minor temperature differences exist in the rest of the cavity due to weak temperature gradients caused by mechanically driven circulations.

REFERENCES

[1] Torrance, K., Davis, R., Eike, K., Gill, P., Gutman, D.,

- Hsui, A., Lyons, S., Zien, H. (1972). Cavity flows driven by buoyancy and shear. *Journal of Fluid Mechanics*, 51(2): 221-231. <https://doi.org/10.1017/S0022112072001181>
- [2] Koseff, J.R., Street, R.L. (1984). The LID-driven cavity flow: A synthesis of qualitative and quantitative observations. *Journal of Fluids Engineering*, 106(4): 390-398. <https://doi.org/10.1115/1.3243136>
- [3] Morzynski, M., Popiel, C.O. (1988). Laminar heat transfer in a two-Dimensional cavity covered by a moving wall. *Numerical Heat Transfer*, 13(2): 265-273. <https://doi.org/10.1080/10407788808910004>
- [4] Moallemi, M.K., Jang, K.S. (1992). Prandtl number effects on laminar mixed convection heat transfer in a lid-Driven cavity. *International Journal of Heat and Mass Transfer*, 35(8): 1881-1892. [https://doi.org/10.1016/0017-9310\(92\)90191-t](https://doi.org/10.1016/0017-9310(92)90191-t)
- [5] Iwatsu, R., Hyun, J.M., Kuwahara, K. (1992). Numerical simulation of flows driven by a torsionally oscillating lid in a square cavity. *Journal of Fluids Engineering*, 114(2): 143-151. <https://doi.org/10.1115/1.2910008>
- [6] Iwatsu, R., Hyun, J.M., Kuwahara, K. (1993). Mixed convection in a driven cavity with a stable vertical temperature gradient. *International Journal of Heat and Mass Transfer*, 36(6): 1601-1608. [https://doi.org/10.1016/s0017-9310\(05\)80069-9](https://doi.org/10.1016/s0017-9310(05)80069-9)
- [7] Prasad, A.K., Koseff, J.R. (1996). Combined forced and natural convection heat transfer in a deep lid-Driven cavity flow. *International Journal of Heat and Fluid Flow*, 17(5): 460-467. [https://doi.org/10.1016/0142-727x\(96\)00054-9](https://doi.org/10.1016/0142-727x(96)00054-9)
- [8] Fedorov, A.G., Viskanta, R. (2000). Three-dimensional conjugate heat transfer in the microchannel heat sink for electronic packaging. *International Journal of Heat and Mass Transfer*, 43(3): 399-415. [https://doi.org/10.1016/s0017-9310\(99\)00151-9](https://doi.org/10.1016/s0017-9310(99)00151-9)
- [9] Stanish, M.A., Schajer, G.S., Kayihan, F. (1986). A mathematical model of drying for hygroscopic porous media. *AIChE Journal*, 32(8): 1301-1311. <https://doi.org/10.1002/aic.690320808>
- [10] Ideriah, F.J.K. (1980). Prediction of turbulent cavity flow driven by buoyancy and shear. *Journal of Mechanical Engineering Science*, 22(6): 287-295. https://doi.org/10.1243/jmes_jour_1980_022_054_02
- [11] Hussien, A.A., Al-Kouz, W., El Hassan, M., Janvekar, A.A., Chamkha, A.J. (2021). A review of flow and heat transfer in cavities and their applications. *The European Physical Journal Plus*, 136(4): 353. <https://doi.org/10.1140/epjp/s13360-021-01320-3>
- [12] Vafai, K., Tien, C. (1981). Boundary and inertia effects on flow and heat transfer in porous media. *International Journal of Heat and Mass Transfer*, 24(2): 195-203. [https://doi.org/10.1016/0017-9310\(81\)90027-2](https://doi.org/10.1016/0017-9310(81)90027-2)
- [13] Khanafer, K.M., Chamkha, A.J. (1999). Mixed convection flow in a lid-Driven enclosure filled with a fluid-saturated porous medium. *International Journal of Heat and Mass Transfer*, 42(13): 2465-2481. [https://doi.org/10.1016/s0017-9310\(98\)00227-0](https://doi.org/10.1016/s0017-9310(98)00227-0)
- [14] Aldoss, T.K., Chen, T.S., Armaly, B.F. (1993). Nonsimilarity solutions for mixed convection from horizontal surfaces in a porous medium-Variable surface heat flux. *International Journal of Heat and Mass Transfer*, 36(2): 463-470. [https://doi.org/10.1016/0017-9310\(93\)80021-l](https://doi.org/10.1016/0017-9310(93)80021-l)

- [15] Chamkha, A.J., Rashad, A.M., Armaghani, T., Mansour, M.A. (2017). Effects of partial slip on entropy generation and MHD combined convection in a lid-Driven porous enclosure saturated with a Cu-Water nanofluid. *Journal of Thermal Analysis and Calorimetry*, 132(2): 1291-1306. <https://doi.org/10.1007/s10973-017-6918-8>
- [16] Bondarenko, D.S., Sheremet, M.A., Oztop, H.F., Abu-Hamdeh, N. (2018). Mixed convection heat transfer of a nanofluid in a lid-Driven enclosure with two adherent porous blocks. *Journal of Thermal Analysis and Calorimetry*, 135(2): 1095-1105. <https://doi.org/10.1007/s10973-018-7455-9>
- [17] Mohan, C.G., Satheesh, A. (2015). The numerical simulation of double-Diffusive mixed convection flow in a Lid-Driven porous cavity with magnetohydrodynamic effect. *Arabian Journal for Science and Engineering*, 41(5): 1867-1882. <https://doi.org/10.1007/s13369-015-1998-x>
- [18] Chamkha, A.J., Rashad, A.M., Mansour, M.A., Armaghani, T., Ghalambaz, M. (2017). Effects of heat sink and source and entropy generation on MHD mixed convection of a Cu-Water nanofluid in a lid-Driven square porous enclosure with partial slip. *Physics of Fluids*, 29(5). <https://doi.org/10.1063/1.4981911>
- [19] Oztop, H.F. (2006). Combined convection heat transfer in a porous lid-Driven enclosure due to heater with finite length. *International Communications in Heat and Mass Transfer*, 33(6): 772-779. <https://doi.org/10.1016/j.icheatmasstransfer.2006.02.003>
- [20] Kandaswamy, P., Muthamilselvan, M., Lee, J. (2008). Prandtl number effects on mixed convection in a Lid-Driven porous cavity. *Journal of Porous Media*, 11(8): 791-801. <https://doi.org/10.1615/jpormedia.v11.i8.70>
- [21] Basak, T., Roy, S., Sharma, P.K., Pop, I. (2008). Analysis of mixed convection flows within a square cavity with uniform and non-Uniform heating of bottom wall. *International Journal of Thermal Sciences*, 48(5): 891-912. <https://doi.org/10.1016/j.ijthermalsci.2008.08.003>
- [22] Karimipour, A., Nezhad, A.H., Behzadmehr, A., Alikhani, S., Abedini, E. (2011). Periodic mixed convection of a nanofluid in a cavity with top lid sinusoidal motion. *Proceedings of the Institution of Mechanical Engineers Part C Journal of Mechanical Engineering Science*, 225(9): 2149-2160. <https://doi.org/10.1177/0954406211404634>
- [23] Maghsoudi, P., Siavashi, M. (2018). Application of nanofluid and optimization of pore size arrangement of heterogeneous porous media to enhance mixed convection inside a two-Sided lid-Driven cavity. *Journal of Thermal Analysis and Calorimetry*, 135(2): 947-961. <https://doi.org/10.1007/s10973-018-7335-3>
- [24] Muthamilselvan, M., Das, M.K., Kandaswamy, P. (2010). Convection in a lid-Driven heat-Generating porous cavity with alternative thermal boundary conditions. *Transport in Porous Media*, 8(2): 337-346. <http://dx.doi.org/10.1007/s11242-009-9429-7>
- [25] Chattopadhyay, A., Pandit, S.K., Sarma, S.S., Pop, I. (2015). Mixed convection in a double lid-Driven sinusoidally heated porous cavity. *International Journal of Heat and Mass Transfer*, 93: 361-378. <https://doi.org/10.1016/j.ijheatmasstransfer.2015.10.010>
- [26] Rajarathinam, M., Nithyadevi, N., Chamkha, A.J. (2017). Heat transfer enhancement of mixed convection in an inclined porous cavity using Cu-water nanofluid. *Advanced Powder Technology*, 29(3): 590-605. <https://doi.org/10.1016/j.appt.2017.11.032>
- [27] Alsabery, A.I., Sheremet, M.A., Chamkha, A.J., Hashim, I. (2019). Impact of nonhomogeneous nanofluid model on transient mixed convection in a double lid-driven wavy cavity involving solid circular cylinder. *International Journal of Mechanical Sciences*, 150: 637-655. <https://doi.org/10.1016/j.ijmecsci.2018.10.069>
- [28] Tiwari, R.K., Das, M.K. (2006). Heat transfer augmentation in a two-Sided lid-Driven differentially heated square cavity utilizing nanofluids. *International Journal of Heat and Mass Transfer*, 50(9-10): 2002-2018. <https://doi.org/10.1016/j.ijheatmasstransfer.2006.09.034>
- [29] Bagai, S., Kumar, M., Patel, A. (2020). Mixed convection in four-Sided lid-Driven sinusoidally heated porous cavity using stream function-Vorticity formulation. *SN Applied Sciences*, 2(12). <https://doi.org/10.1007/s42452-020-03815-7>
- [30] Bagai, S., Kumar, M., Patel, A. (2021). Mixed convection in a two-sided and four-sided lid-driven square porous cavity. *International Journal of Heat and Technology*, 39(3): 711-726. <https://doi.org/10.18280/ijht.390305>
- [31] Mondal, M.K., Biswas, N., Manna, N.K. (2019). MHD convection in a partially driven cavity with corner heating. *SN Applied Sciences*, 1: 1-19. <https://doi.org/10.1007/s42452-019-1712-9>
- [32] Nield, D.A., Bejan, A. (2006). *Convection in Porous Media*. New York: Springer, USA, 629-982. <https://doi.org/10.1007/978-3-319-49562-0>
- [33] Ferziger, J.H., Peric, M. (2001). *Computational Methods for Fluid Dynamics*. 3rd Rev. Ed., Springer, Verlag: Berlin. <https://doi.org/10.1007/978-3-319-99693-6>
- [34] Patankar, S.V. (1980). *Numerical Heat Transfer and Fluid Flow*. Hemisphere Publishing Corporation: Washington.
- [35] Hassinet, L., Si-Ameur, M. (2019). Numerical study on natural convection in a porous cavity that is partially heated and cooled by sinusoidal temperature at vertical walls. *Journal of Porous Media*, 22(1): 73-85. <https://doi.org/10.1615/jpormedia.2019018275>

NOMENCLATURE

a,b	extremities of Lid Moving Part
Da	Darcy number
Gr	Grashof number
g	Gravitational acceleration [ms^{-2}]
K	Permeability of the porous medium [m^2]
K_{eff}	Effective thermal conductivity [$\text{Wm}^{-1} \text{K}^{-1}$]
L_0	Length of the square cavity's side [m]
l_p	Length of the moving part [m]
L_p	Dimensionless length of the moving part
Nul	Local Nusselt number
Nu_{avg}	Average Nusselt number
p	Pressure [Pa]
P	Dimensionless pressure
U_0	Velocity of the moving part [ms^{-1}]
Pr	Prandtl number
Re	Reynolds number
T	Temperature [K]
Ri	Richardson number

u	Fluid velocity in x direction [ms^{-1}]
v	Fluid velocity in y direction [ms^{-1}]
U	dimensionless fluid velocity in x direction
V	dimensionless fluid velocity in y direction

Greek symbols

α	Thermal diffusivity [m^2s^{-1}]
β	Thermal expansion coefficient [K^{-1}]
μ	Dynamic viscosity [$\text{kg m}^{-1} \text{s}^{-1}$]
ν	Kinematic viscosity [$\text{m}^2 \text{s}^{-1}$]
ρ	Density [kg m^{-3}]
θ	Dimensionless temperature
ψ	Dimensionless stream function
ζ	Vorticity

Subscripts

avg	Average
c	Cold
h	Hot
L	Left
M	Middle
R	Right
max	maximum
min	Minimum
m,m	Minimum and maximum